Bangladesh J. Bot. **47**(3): 397-404, 2018 (September)

SIMULATION OF THE PENETRATION RANGE DISTRIBUTION FOR LOW ENERGY IONS INJECTED INTO PLANT SEEDS

WANG LINXIANG*

College of Physics and Electronic Engineering, Xinjiang Normal University, Urumqi 830054, China

Keywords: Simulation, Penetration range distribution, Plant seed, Ion implantation, Monte-Carlo

Abstract

In the present experiment on low-energy ions implanted into seeds, factors such as the unique microstructure of the seeds, the energy and injection mode of the ions, the step diameter and scattering angle of the ions after collision, and the collision energy loss between ions and atomic nuclei or electrons are considered. A modified model for ions implanted into seeds is established. The range distribution is simulated for vanadium, titanium, and iron ions (V^+, Ti^+, and Fe^+) with different energies and injection modes implanted into peanut, cotton, and wheat seeds, using the FORTRAN programming language and Monte-Carlo method; the results are in good agreement with the experimental data. In addition, the model is used to estimate the range distribution for nitrogen, hydrogen, and argon ions (N^+, H^+, Ar^+) implanted into peanut, cotton and wheat seeds.

Introduction

Cell mutagenicity effects caused by ions implanted into plant seeds have been the topic of considerable research (Si *et al.* 2012, Huang *et al.* 2014, Cao *et al.* 2015, Wang *et al.* 2013, Lara *et al.* 2015, Guo *et al.* 2015, Li *et al.* 2015). The physical mechanism of the seed mutagenic effects focuses on the range distribution of ions implanted into the seeds. The TRIM program is only suitable for penetration range calculations for dense and homogeneous target materials (Lindhard and Winther 1964). However, the plant seed is a specific low density, non-uniform target material with many microholes. Therefore, a new calculation model needs to be established for the range distribution of ions implanted into plant seeds. Based on previous work in the literature (Wang *et al.* 2005, 2010 and 2011), various factors are considered, such as the unique microstructure of the seeds, the energy and injection mode of ion implantation, the step diameter and scattering angle of the ions after collision, and the collision energy loss between ions and atomic nuclei or electrons. Following these considerations, a theoretical hypothesis is proposed and a new calculation method is established. The range distribution is calculated for V^+, Ti^+, Fe^+, N^+, H^+, and Ar^+ ions with different energies and fluxes implanted into peanut, cotton, and wheat seeds. The calculated results are compared with the experimental data and discussed.

Materials and Methods

The function (Wang *et al.* 2011) of the nuclear collision energy loss calculated by the TRIM program is modified. The nuclear collision energy loss $(\mathrm{d}E/\mathrm{d}x)_n$ is shown in Table 1. The parameter A is expressed as follows:

$$A=\left(2\pi\right)^{1/2}\cdot\sigma\cdot\alpha\cdot\exp\left[-(\lg\beta-u)^2/(2\sigma^2)\right]\} \qquad (1)$$

*Author for correspondence: <wanglinxiang23@126.com>.

Table 1. Parameters of the nuclear collision energy loss for ions and nuclei in seeds.

Ions	Atomic number Z_1 and average mass number M_1 for ions	Seed	The nuclear collision energy loss $(\mathrm{d}E/\mathrm{d}x)_n$	Parameter α	Parameter β
V^+	$Z_1 = 23$, $M_1 = 50.94$	Peanut	$\rho(L)\cdot 10^9\{-0.513+1.54\times 10^4/A\}$	$0.74E+0.65$	$0.74E+0.65$
Ti^+	$Z_1 = 22$, $M_1 = 47.95$	Peanut	$\rho(L)\cdot 10^9\{-0.513+1.54\times 10^4/A\}$	$0.74E+0.65$	$0.74E+0.65$
		Cotton	$\rho(L)\cdot 10^9\{-0.6885+1.51\times 10^4/A\}$	$0.795E+0.8$	$0.795E+0.8$
Fe^+	$Z_1 = 26$, $M_1 = 55.8$	Peanut	$\rho(L)\cdot 10^9\{-0.513+1.54\times 10^4/A\}$	$0.74E+0.65$	$0.74E+0.65$
		Cotton	$\rho(L)\cdot 10^9\{-0.6885+1.51\times 10^4/A\}$	$0.795E+0.8$	$0.795E+0.8$
		Wheat	$\rho(L)\cdot 10^9\{0.84+1.2\times 10^4/A\}$	$0.81E+0.23$	$0.81E+0.23$
N^+	$Z_1 = 7$, $M_1 = 14$	Peanut	$\rho(L)\cdot 10^7\{-0.513+1.54\times 10^4/A\}$	$0.74E+2.65$	$76.9E+0.65$
		Cotton	$\rho(L)\cdot 10^7\times 5\times 0.889\{0.62\times 10^4/A\}$	$0.68E+1.7$	$12.9E+4.15$
		Wheat	$\rho(L)\cdot 10^7\{0.84+1.2\times 10^4/A\}$	$0.81E+0.23$	$0.81E+0.23$
H^+	$Z_1 = 1$, $M_1 = 1$	Wheat	$\rho(L)\cdot 10^7\{0.84+1.2\times 10^4/A\}$	$0.81E+0.23$	$0.81E+0.23$
Ar^+	$Z_1 = 18$, $M_1 = 40$	Wheat	$\rho(L)\cdot 10^7\{0.84+1.2\times 10^4/A\}$	$0.81E+0.23$	$0.81E+0.23$

where u and σ are correction parameters related to ion energy and injection, and the parameters of the nuclear collision energy loss $(\mathrm{d}E/\mathrm{d}x)_n$ are represented by α and β which are presented in Table 1. E is the ion energy, and $\rho(L)$ is the density function. According to the literature (Lindhard and Winther 1964), the energy loss $(\mathrm{d}E/\mathrm{d}x)_e$ of the collisions between implanted ions and the electrons of the target atoms is as follows:

$$(\mathrm{d}E/\mathrm{d}x)_e = NZ_1^{1/5}\frac{0.0793Z_1^{1/2}Z_2^{1/2}(M_1+M_2)^{3/2}}{(Z_1^{2/3}+Z_2^{2/3})^{3/4}M_1^{3/2}M_2^{1/2}}\cdot 10^{-15}E^{1/2} \qquad (2)$$

where, Z_1 is atomic number of the ion, M_1 is the average mass number of the ion, Z_2 is average atomic number of the seed, M_2 is the average mass number of the seed, N is the average number of target atoms per unit volume, and E is the incident energy. By comparing this with the experimental data, the total collision energy loss correction factor w was determined. The range of the implantation ions R_x can then be calculated using the total collision energy loss as follows:

$$R_x = \int_0^{E_0}\frac{\mathrm{d}E}{-w\cdot[(\mathrm{d}E/\mathrm{d}x)_n+(\mathrm{d}E/\mathrm{d}x)_e)]} \qquad (3)$$

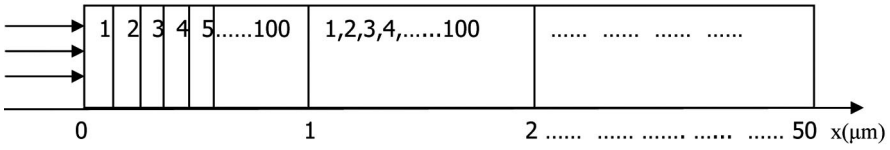

Fig. 1. Target model for the seed.

Based on the model in the literature (Wang *et al.* 2005, 2010 and 2011) and considering the interaction between ions and atomic nuclei in the seed, the target is divided into 5000 layers

starting from the injection surface with a layer spacing of 0.01 μm, with the interval density function $\rho(L)$ along the direction of the injection surface. The target model is presented in Fig. 1.

Assuming only direct interaction between the ions and atoms in the seeds, the nuclear collision energy loss function in the literature (Wang *et al.* 2011) needs to be modified. The nuclear collision energy loss is shown in Table 1. The target density function $\rho(L)$ is expressed as follows:

$$\rho(L) = \rho(Y_z)_{\max} \cdot fa \qquad (4)$$

where ρ_0 is the average target density, N_A is Avogadro's constant, M_2 is the average quality number of targets, Δ_z is the atomic percentage, and Y_z is the atomic mass of C, H, O and N atoms. The other parameters are listed in Table 2 (Wang *et al.* 2005, Wang *et al.* 2010, 2011 and 1987, Lu 2005).

In general, the microstructures of the different seed target materials differ in terms of atomic density, atomic species, and micropore distribution. The range, scattering angle, and energy loss of the ions are also different after the collision between the ions and target atoms. Therefore, the step length $\Delta l \cdot fa_1$ after ion collision is random in the range $0 - 10^{-8}$ m (average atomic spacing of approximately $10^{-9} - 10^{-8}$ m). Secondly, under the two-dimensional assumption, the direction cosine of the ion scattering angle after each collision is $\cos((\pm\pi/2)\cdot fa_2)$. Thirdly, the energy loss $w\cdot[(dE/dx)\cdot\Delta x]\cdot fa_3$ is random after each collision. It is assumed that the target density is constant within the same 0.01 μm interval, and the target density of the different intervals varies in the range $0\text{-}\rho(Y_z)_{\max}$. Where f_a is a pseudo-random number uniformly distributed from 0 to 1; thus, the density $\rho(L)$ of different layers in the target is given by a pseudo-random number between 0 and $\rho(Y_z)_{\max}$. In comparison, the maximum value $\rho(Y_z)_{\max}$ of the density is obtained using Equation (5).

$$\rho(Y_z)_{\max} = MAX\left\{\frac{\rho_0 N_A}{M_2}\Delta_z \cdot Y_z\right\} \qquad (5)$$

The parameters fa_1, fa_2, fa_3, and fa in the above formulas are uniformly pseudo-random numbers in the range 0 - 1. Finally, it is assumed that only direct interaction exists between the implanted ions and target atoms, ignoring secondary and other effects. Based on the above assumptions, the ions can be tracked, the number of ions per 1 μm of thickness can be recorded, and the distribution range for the ions implanted into the seeds can be obtained along the injection direction. The calculation flow is shown in Fig. 2, T and F in the figure represent true and false, respectively.

Results and Discussion

The transport processes of the implanted ions are simulated using the Monte-Carlo method (Wen *et al.* 2012). The relationship between the position x_{J+1} and the energy $E_{J+1}(x_{J+1})$ of the ions is given by using the FORTRAN programming language, pseudo-random numbers in the range from 0 – 1 are obtained by calling auxiliary functions (William 1997). Under the conditions of the modified model and theoretical assumptions, this calculation program is used to obtain the range distributions of different ions implanted into different seeds, as shown in Fig. 3.

$$x_{J+1} = x_J + (\Delta l \cdot fa_1) \cdot \cos((\pi/2) \cdot fa_2) \quad (6)$$

$$E_{J+1}(x_{J+1}) = E_J(x_J) - [(dE/dx)_J \cdot \Delta x_J] \cdot fa_3 \quad (7)$$

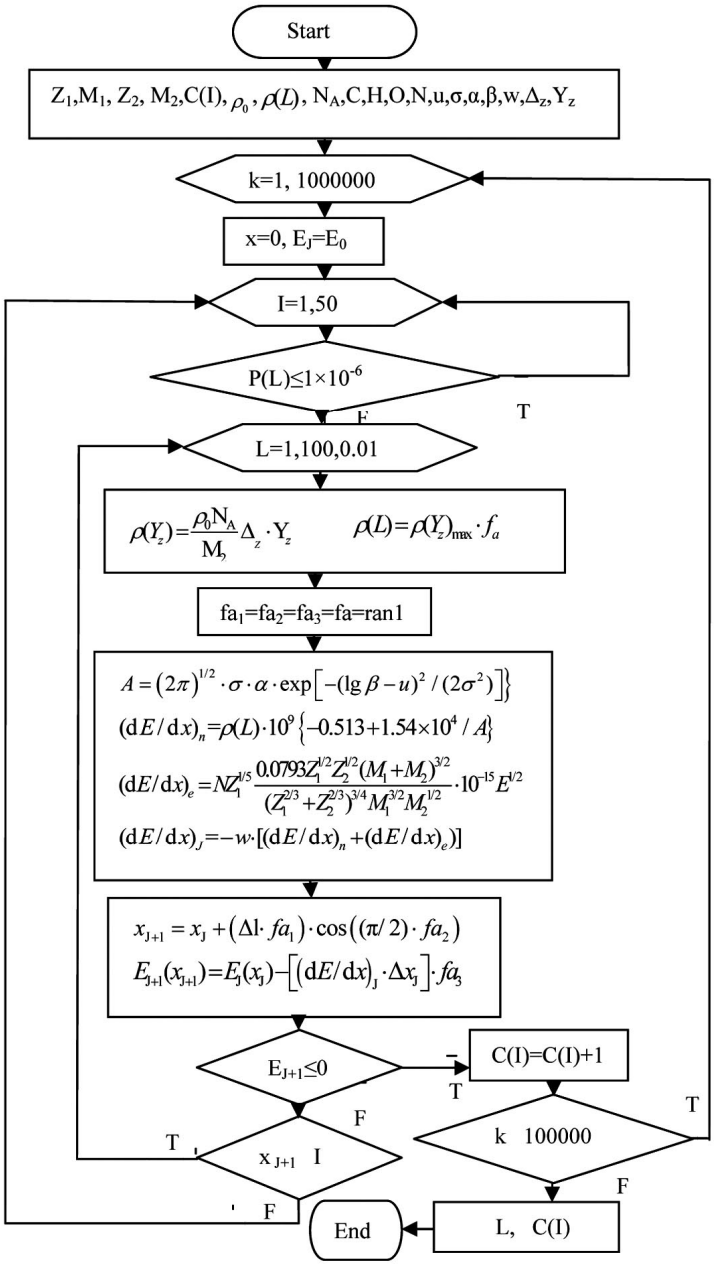

Fig. 2. Simulation flow chart for ions implanted in different seeds.

Table 2. Parameters for V^+, Ti^+, Fe^+, N^+, H^+, and Ar^+ ions implanted in the seeds with different energies and flux.

Seed	Atomic number Z_2, the average mass number M_2 for seed, and density ρ_0(g/cm^3)	Atomic percentage of C, H, O, N	Ions	The initial position (μm) and the initial energy (keV)	Fluence (ions/cm^2)	u, σ parameter
Peanut	Z_2 = 3.19, M_2 = 5.79, ρ_0 = 1.1002	0.3175 0.5940 0.0125 0.0759	V^+	x_0 = 0, E_0 = 200	9×10^{16}	u = 2.67, σ = 10.8
			Ti^+	x_0 = 0, E_0 = 20	2×10^{17}	u = 2.80, σ = 11.37
			Fe^+	x_0 = 0, E_0 = 110	2×10^{16}	u = 2.44, σ = 9.02
			N^+	x_0 = 0, E_0 = 20	2×10^{17}	u = 2.80, σ = 11.37
Cotton	Z_2 = 3.25, M_2 = 5.0, ρ_0 = 1.4838	0.3076 0.5864 0.0765 0.0295	Ti^+	x_0 = 0, E_0 = 20	2×10^{17}	u = 2.80, σ = 11.37
			Fe^+	x_0 = 0, E_0 = 110	2×10^{16}	u = 2.44, σ = 9.02
			N^+	x_0 = 0, E_0 = 20	2×10^{17}	u = 2.80, σ = 11.37
Wheat	Z_2 = 4.1, M_2 = 7.7, ρ_0 = 1.32	0.4444 0.0617 0.4938 0.0001	Fe^+	x_0 = 0, E_0 = 110	5×10^{16}	u = 2.27, σ = 9.76
			Fe^+	x_0 = 0, E_0 = 110	10^{17}	u = 2.20, σ = 12.04
			Fe^+	x_0 = 0, E_0 = 20	10^{17}	u = 2.29, σ = 14.04
			N^+	x_0 = 0, E_0 = 20	2×10^{17}	u = 2.80, σ = 11.37
			H^+	x_0 = 0, E_0 = 20	10^{17}	u = 2.29, σ = 14.04
			N^+	x_0 = 0, E_0 = 20	10^{17}	u = 2.29, σ = 14.04
			Ar^+	x_0 = 0, E_0 = 20	10^{17}	u = 2.29, σ = 14.04

All the curves have been normalized. The most probable range is taken as the location with the maximum probability of ions. Fig. 3 a-g shows the results of systematic simulations and experimental measurements of the range distributions for V^+, Ti^+, and Fe^+ ions implanted into peanut, cotton, and wheat. The basic distributions, trends, and trailing edges of the curves are consistent with the experimental results, but for the range from 0 - 2 μm, there is a relatively large discrepancy between the computational and experimental results. Some possible reasons for this disagreement are mentioned in the literature (Wang *et al.* 2010). In addition, this model ignores secondary effects, charge transfer, and the cascading effect of ions implanted in seeds, and therefore has room for modification and improvement. Compared to the computational model in the literature (Wang *et al.* 2011), the present model is more realistic, owing to its consideration of the randomness of the target layer density. The results from the present model are closer to experimental values. Fig. 3 h-i shows the systematic simulation results for the range distributions of N^+, H^+, and Ar^+ ions implanted into peanuts, cotton, and wheat.

Table 3 lists experimental results (Lu *et al.* 2005, Wang *et al.* 2002, Yang 2005, Wei *et al.* 2003) and the simulation results (Wang and Wang 2005, 2011) from one dimensional model and two dimensional model, as well as the simulation results from this work. Obviously, the effects of different injection methods on the ion distribution may exceed the effects of the energy.

From Fig. 3 and Table 3, it appears that the energies and ion fluxes are all same, and that when the average target density is higher, the most probable range and the maximum range are smaller. For the same target material, the same energy, and the same ion, when the flux of ions increases, the maximum range also increases. Therefore, the ion penetration range distribution is affected by several experimental factors, including the energy, fluence, and injection mode, which in particular requires further research.

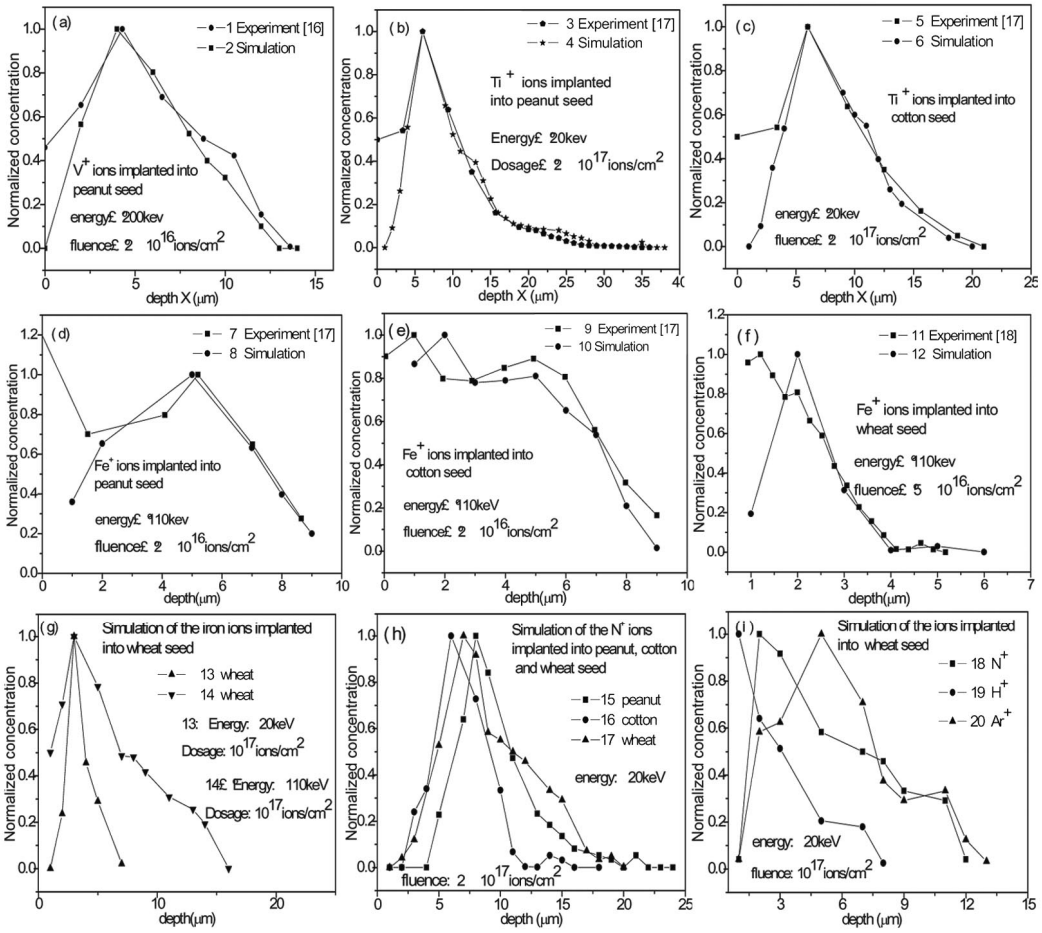

Fig. 3. Penetration range distribution of ions implanted in different seed types with different energies and fluxes.

The most probable range and the maximum range calculated in this work for V^+, Ti^+, and Fe^+ ions implanted into peanut, cotton and wheat seeds are consistent with experimental results, and are closer to those measured for the pulse injection mode. The penetration range distribution is also estimated using this model for the injection of N^+, H^+, and Ar^+ ions into peanut, cotton, and wheat seeds by the pulse injection mode. By comparing with the model in the literature (Wang *et al.* 2005, 2010 and 2011), various influencing factors are identified, such as the ion energy, fluence, injection mode, random step diameter of ions, random scattering angle, and inhomogeneity of the plant seed. This simulation model is closer than previous models to the actual situation for ions implanted into seeds. If the secondary effects of ion implantation are taken into account, this model can be further modified and improved.

Taking into consideration the unique microstructure of plant seeds, a microscopic model of the seed material and an operational flow are designed using the FORTRAN programming language. The range distribution is simulated for V^+, Ti^+, and Fe^+ ions with different energies and

Table 3. Comparison of the penetration range for ions implanted in the different seed with different energies and flux; (a) low beam scanning injection, (b) intense beam pulse injection.

Ion	Energy (keV)	Fluence (ions/cm^2)	Injection method	Seed	Experiment and simulation	Most probable range (μm)	Maximum range (μm)
V^+	200	9×10^{16}	(a)	Peanut	Experiment	4.25	13.6
					One dimensional model	6.0	13.0
					Two dimensional model	4	14
					Simulation	4	14
Ti^+	20	2×10^{17}	(b)	Peanut	Experiment	9	36
					TRIM calculation	0.24	-
					One dimensional model	6	38
					Two dimensional model	9	34
					Simulation	9	36
Ti^+	20	2×10^{17}	(b)	Cotton	Experiment	6.0	21
					TRIM calculation	0.0293	-
					One dimensional model	6	18
					Two dimensional model	6	26
					Simulation	6	20
Fe^+	110	2×10^{16}	(a)	Peanut	Experiment	5.2	8.66
					Simulation	5	9
	110	2×10^{16}	(a)	Cotton	Experiment	1	8
					Simulation	2	9
	110	5×10^{16}	(a)	Wheat	Experiment	0.935	5
					Simulation	2	6
	110	10^{17}	(a)	Wheat	"	3	16
	20	10^{17}	(a)	Wheat	"	3	7
N^+	20	2×10^{17}	(b)	Peanut	"	8	24
	20	2×10^{17}	(b)	Cotton	"	6	18
	20	2×10^{17}	(b)	Wheat	"	7	20
N^+	20	10^{17}	(b)	Wheat	"	2	12
H^+	20	10^{17}	(b)	Wheat	"	1	8
Ar^+	20	10^{17}	(b)	Wheat	"	5	13

fluxes implanted into peanut, cotton, and wheat seeds, using the Monte-Carlo method. The computational results obtained from this model are closer to experimental values than those obtained from the previous model. Moreover, this model is used to estimate the range distribution of N^+, H^+, and Ar^+ ions in peanut, cotton, and wheat seeds, thus demonstrating that it provides a new method to calculate the range distribution for ions with low energy implanted into plant seeds.

Acknowledgements

The author is grateful for financial support from the research foundation of Xinjiang Normal University Laboratory of Novel Light Source and Micro/Nano-Optics (XJNUSYS092017B04) for this study.

References

Aluora SK 1987. Chemistry and Biochemistry of the Bean. Translated by Gao Jian. Beijing: Science Publication.

Cao G, Zhang M and Miao J 2015. Effects of X-ray and carbon ion beam irradiation on membrane permeability and integrity in saccharomyces cerevisiae cells. Journal of Radiation Research **56**: 294-304.

Guo XP, Zhang MM and Miao JS 2015. Research hotspots and recent progress of biological effects induced by heavy ion beam irradiation. Journal of Radiation Research and Radiation Processing, **33**(4): 040102.

Huang HY, Zhang JD and Du N 2014. Biological effect of maize seed by different N^+ ion. Seed **33**(1): 37-39.

Lara PC, López Pealver JJ and de Araújo Farias V 2015. Direct and bystander radiation effects: A biophysical model and clinical perspectives. Cancer Letters **356**(1): 5-16.

Li J, Zhang X and Dong AX 2015. Study of biological effect of ion implantation on salvia splendens. Journal of Nuclear Agricultural Sciences **29**(7): 1302-1306.

Lindhard J, Aa Winther and Mat. Fys 1964. Medd. Dan. Vid. Selsk **34**(4): 1-22.

Lu T, Zhou HY and Ding XJ 2005. The study of depth distribution for ion with low energy implanted into plant seeds and mechanism of biological effect. Acta Phys. Sin. **54**(10): 4822-4826.

Si J, Zhang H and Wu ZH 2012. Applications and research progress of plant breeding with ion implantation technique. Journal of Radiation Research and Radiation Processing **30**(6): 321-327.

Wang LX and Wang SH 2005. Calculation of the Penetration depth and concentration distribution for vanadium ions with low energy implanted into the peanut seed using Monte-Carlo method. Journal of Xinjiang University (Natural Science Edition) **22**(2): 172-177.

Wang LX and Wang SH 2010. Simulation of depth-concentration distribution for 20keV titanium ions implanted into seed. Journal of Atomic and Molecular Physics **27**(05): 954-962.

Wang LX and Wang SH 2011. Simulation of the depth- concentration distribution for low energy ions implanted into Seed. Journal of Nuclear Agricultural Science **25**(5): 0886-0891.

Wang XF, Lu T and Zhou HY 2002. Study of penetration depth for V^+ with low energy implanted in peanut seeds. Atomic Energy Science and Technology **36**(6): 531-534.

Wang YL and Wang WD 2013. SEM of the Wheat Seed's Surface Cell Implanted by KeV Ion Beam. Chinese Journal of Spectroscopy Laboratory **30**(5): 2141-2145.

Wen DZ, Zhuo RH and Ding DJ 2012. Generation of correlated pseudorandom variables in Monte-Carlo simulation. Acta Phys. Sin. **61**(22): 220204-1-7.

William H Press 1997. Numerial recipes in Fortran 77: the art of scientific computing. Beijing: Library of congress cataloguing in Publication Data.

Wei ZQ, Yuan SB and Xie HM 2003. Range distribution of low energy ions implanted into embryo of wheat seed. Journal of Nuclear Physics Review **20**(3): 218-221.

Yang HL 2005. Study on the physical mechanism for ions with low energy implanted into cotton seeds. Xinjiang University Master Thesis, pp. 32-38.

(Manuscript received on 27 May, 2017; revised on 13 December, 2017)